REVIEW OF MODEL SENSOR STUDIES ON $Pd/SnO_2(110)$ SURFACES

Teresa B. Fryberger and Steve Semancik
Chemical Process Metrology Division
National Institute of Standards and Technology
Gaithersburg, Maryland

SUMMARY

In this paper, studies performed at the National Institute of Standards and Technology on the model gas sensor system, $Pd/SnO_2(110)$, are reviewed. Adsorption and interfacial effects play a primary role in the gas sensing process, as they do in catalysis. For this reason, we have used a variety of surface sensitive techniques in our research, including x-ray and ultraviolet photoelectron spectroscopies (XPS and UPS), low energy electron diffraction (LEED), and ion scattering spectroscopy (ISS). By combining these complementary techniques with in situ gas response (conductance) measurements, we have been able to correlate directly sensor activity with the composition and structure of the Pd/SnO_2 interface. Although the intent of this work is develop an understanding of gas sensing mechanisms, its relevance to Pt/SnO_2 catalytic systems is obvious.

INTRODUCTION

The electrical conductivity of a semiconducting metal oxide like tin oxide (SnO_2) can be altered by adsorption of gases from the ambient. This phenomenon has been applied in gas sensing devices fabricated for detection of combustible and toxic gases such as hydrocarbons, alcohols, H_2, CO and NO_x (ref. 1). Many commercial sensors use semiconducting SnO_2 sintered powders or films to which small amounts of a catalytic metal, such as Pd, have been added to increase sensitivity and selectivity towards specific gases. This type of sensor is essentially identical to a supported catalyst, such as the CO oxidation catalysts discussed in these proceedings. In gas sensing, however, one is interested in obtaining an electrical measure (conductivity change) of the extent that adsorption or reaction occurs, rather than a product yield.

In an attempt to understand the detailed mechanisms involved in gas sensing, and to improve sensing measurements, we have conducted step-wise studies on simplified, crystalline specimens of SnO_2 with and without surface-dispersed catalytic additives. In this paper, we first briefly summarize results on the surface properties of pure $SnO_2(110)$. Second, the interaction between a catalytic additive, Pd, and the $SnO_2(110)$ substrate is discussed. Both the growth mode of vapor-deposited Pd on the surface and the electronic interaction between the metal and the oxide are considered. Although we have investigated the role of substrate defect density on the Pd/SnO_2 interaction, results here are limited primarily to deposition on a nearly ideal, oxidized surface. Third, we report results for hydrogen and oxygen adsorption and coadsorption on the 3 ML $Pd/SnO_2(110)$ model sensor surface. Hydrogen has obvious importance as a gas to be monitored and as a dissociation product of hydrocarbons and alcohols, and oxygen is nearly always abundant in the sensor ambient (often, air). These gases also provide the simplest

reducing and oxidizing environments for understanding mechanistic effects. It is worth noting, however, that the mechanistic effects studied in this work can, to a large extent, be generalized to other oxidizing and reducing gases, with kinetic details being dependent on the particular gas.

EXPERIMENTAL

Model Specimens

In order to isolate various chemical, structural, and additive effects and to more clearly evaluate their roles in gas sensing, we chose single crystal tin oxide samples for our model studies. The (110) face was chosen because it is the most stable, naturally occurring face (ref. 2) and can be expected to be predominant in polycrystalline sensing elements. Thus, studies on (110) crystals are particularly relevant to the local chemical and electronic effects occurring in real SnO_2 sensors. The SnO_2 sample used in this work was cut from a single crystal needle (ref. 3) and was oriented and polished to within 1° of the (110) face.

To investigate the role of a catalytic additive in sensing, we studied both the interaction of palladium with the SnO_2(110) surface and its effect on sensing response. The Pd was deposited under ultrahigh vacuum (UHV) conditions using a filament evaporator to coverages ranging from 0.1 to 30 monolayer equivalents (ML) as measured by a calibrated quartz crystal monitor. All Pd depositions were carried out with the substrate at room temperature.

Analytical Techniques

Since adsorption and interfacial effects play a primary role in gas sensing processes, we used surface-sensitive analytical techniques, all housed in a single vacuum system, in these studies. By using a variety of techniques we are able to monitor surface chemistry (oxide stoichiometry, chemical states of gas and additive adsorbates), atomic structure (crystallite orientation, surface reconstruction), and electronic structure (gap states, band bending, additive-induced density of state changes). In addition, in situ conductance measurements were carried out in order to correlate the model sensor electronic response to the specific changes in chemistry produced by adsorption.

The multi-technique facility used in this study is represented schematically in fig. 1, and is described in refs. 4-5. The system consists of two coupled vacuum chambers that can operate over pressures from 10^{-11} to 10^{3} torr. A translation/rotation stage was used to move samples back and forth between the two chambers, permitting access to instrumentation and test ambients. The results presented here were obtained using XPS, UPS, ISS, LEED, and surface conductance change measurements.

XPS, UPS, and ISS spectra were collected in the analysis chamber of the vacuum system which is based on the VG ESCALAB MK II (ref. 6). Non-monochromatized Mg Kα radiation (1253.6 eV) was used for XPS and an RF discharge lamp was used as a He I (21.2 eV) source for UPS. All photoelectron binding energies were referenced to the Fermi level. For the ISS, a scattering angle of 130° was set by the fixed positions of the ion source and the analyzer. An He^+ or Ne^+ ion beam with a primary energy (E_o) of 1000 eV was used at an incident angle of 50° with respect to the surface normal along the (001) azimuth. All XPS, UPS, and ISS spectra were taken with the sample at room temperature. In situ conductance changes measurements were

made using a retractable, four-point probe similar to one described in detail in ref. 7.

Argon ion bombardment and heating were used to clean and order the surface of the SnO_2(110) crystal, and its condition was monitored by XPS and LEED. The sample mounting and heating arrangements are described in ref. 5. Sample temperatures could be controlled between 300 and 1000K, and were measured by a W5%Re/W26%Re thermocouple in direct contact with one end of the sample. Pure or mixed gases could be introduced at the desired partial pressures (up to 1 atmosphere) from a 12-port gas manifold. The base pressure was $1X10^{-10}$ mbar in both the preparation and the analysis chambers.

RESULTS AND DISCUSSION

In order to understand the detailed mechanisms involved in sensing (or catalysis) it was necessary to investigate model sensors (oxide-supported metals) in a step-wise fashion. That is, we studied 1) the properties of pure tin oxide surfaces; 2) the interaction of Pd with the SnO_2 surface; and 3) adsorption of H_2 and O_2 gases; and 4) coadsorption of these gases on the pure and Pd-dosed surfaces. In the following discussion, results are also presented, more or less, in this order.

Surface Properties of Clean SnO_2(110)

Tin oxide is an n-type semiconductor which, like TiO_2, has a rutile crystal structure. The electrical conductivity of SnO_2 is due to the presence of oxygen vacancy defects, and the creation of oxygen vacancies and defect electronic states at the clean SnO_2(110) surface has therefore been studied in detail (refs. 5,8-10). It has been demonstrated that heating sputtered surfaces in UHV can result in the formation of well-ordered, oxygen deficient surfaces which exhibit (1x1), c(2x2),(4x1), and (1x2) LEED patterns depending upon the annealing temperature (refs. 8,10). In addition, the conductance of the disordered sputtered and ordered surfaces can vary by more than two orders of magnitude(ref. 8).

Cox et al (ref.5) have shown that surfaces with a nearly perfect termination of the rutile (110) plane can be formed by in situ oxidation of oxygen deficient SnO_2(110) at 700K in 1 Torr oxygen. Furthermore, by annealing the oxidized surface in vacuum, oxygen vacancies can be produced and their number density and type can be controlled by the choice of annealing temperature. In this paper, we discuss the effects of Pd when deposited on the nearly stoichiometric, oxidized surface formed by heating the sample at 700K in 1 torr of O_2 for 3 minutes as described in ref. 5. This surface should be most representative of a sensor surface since sensors generally operate under oxidizing conditions (i.e., in air at elevated temperatures).

Palladium Deposition on SnO_2(110)

The interaction of palladium with the nearly perfect, oxidized SnO_2(110) surface was studied by sequential Pd deposition at room temperature (ref. 11). XPS Pd 3d and Sn 3d core levels are plotted in figure 2 as a function of increasing palladium coverage. While the Sn 3d peaks (figure 2a) are increasingly attenuated as the Pd film grows, there are no large binding energy shifts or peak shape changes. This suggests that strong chemical interactions are not occurring between

Pd and surface Sn atoms. Note, however, that at coverages greater than ~8 monolayers (ML), a small shoulder appears on the low binding energy side of the Sn 3d peaks indicating the presence of a small amount of metallic Sn. We believe that this is due to the formation of a Pd-Sn alloy at higher Pd coverages*. Unlike the Sn 3d spectra, the Pd 3d peaks (fig. 2b) show a substantial shift to lower binding energy as Pd coverage increases. The peaks get narrower with increasing Θ_{Pd} (the FWHM goes from 2.10 eV at 0.3 ML to 1.70 eV at >3.0 ML) and by 8.0 ML, both the lineshape and peak position are very similar to those of a palladium foil. This behavior suggests that the palladium film is metallic. A metallic overlayer is consistent with the lack of change in the Sn 3d peaks and the conclusion that most of the Pd does not strongly react with SnO_2. If a sizable amount of Pd reacted strongly with the surface, one would expect it to be at least partially oxidized. Oxidation would lead to core level broadening and/or higher binding energies that are not seen here (see also discussion below).

The weak chemical interaction between Pd and SnO_2 suggested by the XPS results is consistent with a clustering growth mode of the Pd overlayer*. To confirm that clustering of Pd occurs on $SnO_2(110)$, Ne^+ ISS experiments, which probe the top surface layer, were performed at various coverages. The results are shown in figure 3. To avoid effects from surface damage due to the Ne^+ ion beam, ISS spectra were not taken after sequential Pd depositions. Instead, the surface was cleaned, reoxidized, and Pd was deposited to a given coverage before collecting each spectrum. Also, short scanning times were used to minimize beam damage. Since ISS provides qualitative information about the composition of the outermost layer, one would expect the Sn peak to completely disappear within the first few Pd monolayers if layer-by-layer growth occurs. Instead, it is seen in fig. 3, that the Sn signal at $E = 0.58\ E_o$ is not completely attenuated until nearly 10 ML, suggesting that at least some bare substrate patches are present up to that coverage. This implies that initial clustering occurs with lateral growth to fill in the bare patches by <10 ML. Thus, both XPS and ISS results are consistent with growth by clustering.

To determine how the development of the Pd/SnO_2 interface affects the electronic and electrical properties of the composite surface, conductance and the photoelectron intensity at the Fermi level $N(E_F)$ were monitored as Pd was sequentially deposited. Results from these measurements are shown in figure 4. The photoelectron intensity at E_F, measured with UPS, correlates with the occupied density of states at E_F. It is, therefore, a measure of the metallic character of the overlayer. Figure 4 shows that the Fermi level intensity begins to rapidly increase between 1 and 2 monolayers. In contrast, the conductance does not begin to rise significantly until 7-8 ML, where it goes up sharply. The differing behavior between conductance and the $N(E_F)$, both measures of the metallic nature of the overlayer, can also be explained by the clustering growth mode of the Pd film. First, if Pd clusters are formed, one would expect to see the kind of rapid rise in $N(E_F)$ observed at low coverages, as each of the growing islands takes on metallic character. However, at these coverages (< 6 ML), the 4-point measurement is still responsive to the underlying substrate conductance since the Pd, although metallic, is in isolated clusters. As Θ_{Pd} increases and the clusters grow laterally to produce a connected adlayer, conductance should begin to increase; such behavior is observed at 7-8 monolayers. Note that this is in the same coverage range where the substrate Sn peak disappears in ISS (figure 3), indicating that a continuous film has formed.

*T. B. Fryberger and S. Semancik, Surface Science, work in progress.

Model Sensor Response

In general, the conductivity of SnO_2-based sensors increases when exposed to reducing gases (e.g. H_2,CO) and decreases when exposed to oxidizing gases (e.g. O_2). In order to better understand the mechanisms which control these conductivity changes, we have made in situ conductance measurements of the $Pd/SnO_2(110)$ model sensor in both hydrogen and oxygen atmospheres. A Pd coverage of 3 ML was chosen since at this coverage, as discussed previously, the composite surface consists of metallic (catalytic) Pd clusters on the essentially unperturbed tin oxide substrate (previous work* has shown this to be the optimal configuration for electrical response to hydrogen). The 3 ML $Pd/SnO_2(110)$ surface was subjected to a series of consecutive hydrogen and oxygen exposures while monitoring the conductance of the sample, which was held at 400K throughout the experiment (ref. 12). The results are shown in figure 5, where conductance versus time is plotted. The sequence of steps in this experiment was as follows:

1) The sample was held in UHV ($<8 \times 10^{-10}$ mbar) at 400K for several minutes to obtain an initial conductance value. It is seen in figure 1 that there is virtually no drift; the conductance remained constant at 58×10^{-6} A/V.

2) The sample was exposed to a constant pressure (10^{-5} mbar) of hydrogen for 6 minutes. This first hydrogen exposure provides a measure of the model sensor response in the absence of oxygen (both gaseous/ambient and chemisorbed). The conductance increased steadily during exposure to H_2; it increased by 47% after 6 minutes exposure at constant pressure. (Further exposure time results in a slow upward drift in conductance*.)

3) The chamber was evacuated to $<8 \times 10^{-10}$ mbar. Upon evacuation, the conductance decreased but did not return to its initial value, indicating that the interaction between hydrogen and the surface is not fully reversible.

4) The sample was exposed to 10^{-5} mbar of O_2 causing the conductance to decrease to 30% below the starting point (step 1).

5) The chamber was again evacuated to $<8 \times 10^{-10}$ mbar. Upon evacuation of O_2 the conductance did not increase, indicating that the O_2 interaction with the surface is even less reversible at 400K than the hydrogen interaction (step 3).

6) Steps 2-5 were repeated. The total response to H_2 following O_2 exposure and evacuation (step 6) was more than twice as large as the first H_2 response (step 2), where no previous oxygen exposure had occurred. In addition, the total conductance change occurred within a few seconds rather than over several minutes (as seen in the first H_2 exposure), and the response became reversible in the presence of oxygen.

As shown in figure 5 (step 2), exposure of the 3 ML $Pd/SnO_2(110)$ surface to hydrogen results in a nearly 50% conductance increase. This can be compared to the small hydrogen response (3% increase) for the bare $SnO_2(110)$ surface (not shown; see ref. 4). The enhancement by Pd is most likely due to a "spillover" mechanism wherein hydrogen molecules dissociate on the catalytic Pd clusters and then diffuse, probably across and/or through the clusters, to the substrate where the

*T. B. Fryberger and S. Semancik, Sensors and Actuators, work in progress.

hydrogen atoms can interact with the semiconducting SnO_2 to increase its conductance. The irreversibility of the response to H_2 at 400K is thought to be due to adsorbed hydrogen remaining on the surface at this temperature (ref. 12).

Figure 5 (steps 4 and 5) also shows that the conductance decreases to well below the starting point (step 1) upon exposure to O_2. It should be pointed out that, as in the case of H_2, the bare substrate shows no response to O_2 at 400K, indicating that the surface is activated toward oxygen by the Pd clusters (ref. 12). Since adsorbed hydrogen is most likely present on the surface (as discussed above), it is probable that chemisorbed oxygen reacts with the hydrogen atoms to form volatile water molecules (refs. 13,14). This would return the conductance only to its initial value (step 1), however. The fact that the conductance decreases an additional 30% suggests that oxygen must adsorb on the surface, in addition to reacting with adsorbed hydrogen (although a small amount of this additional decrease may be due to reaction of oxygen with residual hydrogen in the Pd clusters). It is well established that O_2 dissociates on, but does not oxidize, Pd surfaces in this temperature range (refs. 13-15). It is possible that the response of the Pd/SnO_2 surface toward O_2 is then produced by spillover of chemisorbed oxygen atoms, similar to that occurring for hydrogen. Note that the response to oxygen is even less reversible upon evacuation (step 5) than the response to hydrogen (step 3). This irreversibility is most likely due to the presence of chemisorbed oxygen, which desorbs only above 400K, as in the case of hydrogen.

The results in figure 5 suggest that the 400K response of Pd/SnO_2 to H_2 in the presence of oxygen is, to a large extent, due to reactions of chemisorbed species, both with the surface and with each other. To show that reactions between chemisorbed species are important, He^+ ISS experiments using isotopically labeled oxygen were performed (ref. 12). ISS is particularly useful here because of its top layer sensitivity, allowing qualitative determination of the atomic composition at a sample surface. The results are shown in figure 6 where the oxygen region of the ISS spectrum can be seen for a 3 ML $Pd/SnO_2(110)$ surface (a) before exposure to any gases, (b) after exposure to 10^{-5} mbar of $^{18}O_2$ at 400K, and (c) after exposure of the surface in (b) to 10^{-5} mbar of H_2 at 400K. The spectrum in figure 6a represents the surface lattice oxygen signal since no gas exposures have been performed. It is seen in figure 6b that ^{18}O is clearly distinguishable from ^{16}O and that approximately 1/3 of the total signal is due to ^{18}O. When the surface is then exposed to hydrogen (figure 6c), essentially all of the ^{18}O signal is attenuated, indicating that hydrogen preferentially reacts with the ^{18}O. The most likely explanation for this is that ^{18}O is a chemisorbed, rather than a lattice oxygen species. These results provide strong evidence that the reaction

$$2H_{ads} + O_{ads} \longrightarrow H_2O_{gas}$$

is a primary mechanism for the large conductance changes seen in figure 5 (steps 4 and 6). Whether this reaction takes place on the Pd particles, on the SnO_2 substrate, or on the boundaries between the two materials remains to be determined (ref. 12).

CONCLUSIONS

Multi-technique surface analytical studies of Pd-dosed $SnO_2(110)$ samples have been performed in a step-wise manner to investigate the role of catalytic additives in gas sensing. It was found that metallic Pd clusters on a nearly unperturbed SnO_2 substrate can be formed by evaporating Pd onto the well-oxidized, nearly ideal $SnO_2(110)$ surface at room temperature. By combining the surface techniques with

electrical gas response measurements, we showed that, at 400K, the response of the sensor to H_2, in the presence of O_2, is dominated by the water forming reaction between chemisorbed hydrogen and oxygen. Further work will focus on using gas mixtures to simulate more realistic sensing environments. These studies demonstrate the utility of combining basic research tools (e.g. surface science) with simulations of actual operating conditions for understanding the mechanistic aspects of device (e.g. sensor, catalyst) operation.

REFERENCES

1. See, for example, P. K. Clifford, and D. T. Tuma: Characteristics of Semiconductor Gas Sensors II. Transient Response to Temperature Change. Sensors and Actuators, vol. 3, 1982/3, pp. 255-281; J. N. Zemel: Theoretical Description of Gas-Film Interaction on SnO_x. Thin Solid Films, vol. 163, 1988, pp. 139-202; D. Kohl, Surface Processes in the Detection of Reducing Gases with SnO_2-based Devices. Sensors and Actuators, vol. 18, 1989, pp. 71-113.

2. Z. M. Jarzebski and J. P. Morton: Physical Properties of SnO_2 Materials. J. Electrochem. Soc., vol. 123, 1976, pp. 199c-205c.

3. B. Thiel and R. Helbig: Growth of SnO_2 Single Crystals by a Vapour Phase Reaction Method. J. Cryst. Growth, vol. 32, 1976, pp. 259-264. (We thank Professor Helbig for supplying the crystal used in this study.)

4. S. Semancik and T. Fryberger: Model Studies of SnO_2-Based Gas Sensors: Vacancy Defects and Pd Additive Effects. Sensors and Actuators, vol. B1, pp. 97-102, 1990.

5. D. F. Cox, T. B. Fryberger, and S. Semancik: Oxygen Vacancies and Defect Electronic States on the SnO_2(110)-1 x 1 Surface. Phys. Rev., vol. B33, pp. 2072-2083, 1989.

6. Certain commercial instruments are identified in order to adequately specify the experimental procedure. In no case does such identification imply endorsement by the National Institute of Standards and Technology.

7. J. W. Erickson and S. Semancik: An Economical Ultrahigh Vacuum Four-Point Resistivity Probe. J. Vac. Sci. Technol., vol. A5, 1987, pp. 115-117.

8. E. deFresart, J. Darville and J.M. Gilles: Influence of the Surface Reconstruction on the Work Function and Surface Conductance of (110) SnO_2. Appl. Surf. Sci., vol. 11/12, 1982, pp. 637-651.

9. S. Munnix and M. Schmeits: Electronic Structure of Tin Dioxide Surfaces. Phys. Rev., vol. B27, 1983, pp. 7624-7635; Electronic Structure of Point Defects on Oxide Surfaces. Phys. Rev., vol. B33, 1986, pp. 4136-4144.

10. D. F. Cox, T. B. Fryberger, and S. Semancik: Surface Reconstructions of Oxygen-Deficient SnO_2(110). Surf. Sci., vol. 224, pp. 121-142, 1989.

11. T. B. Fryberger, J. W. Erickson, and S. Semancik: Chemical and Electronic Properties of Pd/SnO_2(110) Model Gas Sensors. Surface and Interface Analysis, vol. 14, 1989, pp. 83-89.

12. T. B. Fryberger and S. Semancik: Conductance Response of Pd/SnO_2 (110) Model Gas Sensors to H_2 and O_2. Sensors and Actuators, 1990.

13. L.-G. Petersson, H. M. Dannetun, and I. Lundstrom: Water Production on Palladium in Hydrogen-Oxygen Atmospheres. Surface Science, vol. 163, 1985, pp. 273-284; and references therein.

14. T. Engel and H. Kuipers: A Molecular-Beam Investigation of the Reaction H_2 + 1/2 $O_2 \rightarrow H_2O$ on Pd(111). Surface Science, vol. 90, 1979, pp. 181-196.

15. M. Milun, et al.: Thermal Desorption Spectroscopy of the O_2/Pd(110) System. Surface Science, vol. 211/212, 1989, pp. 887-895.

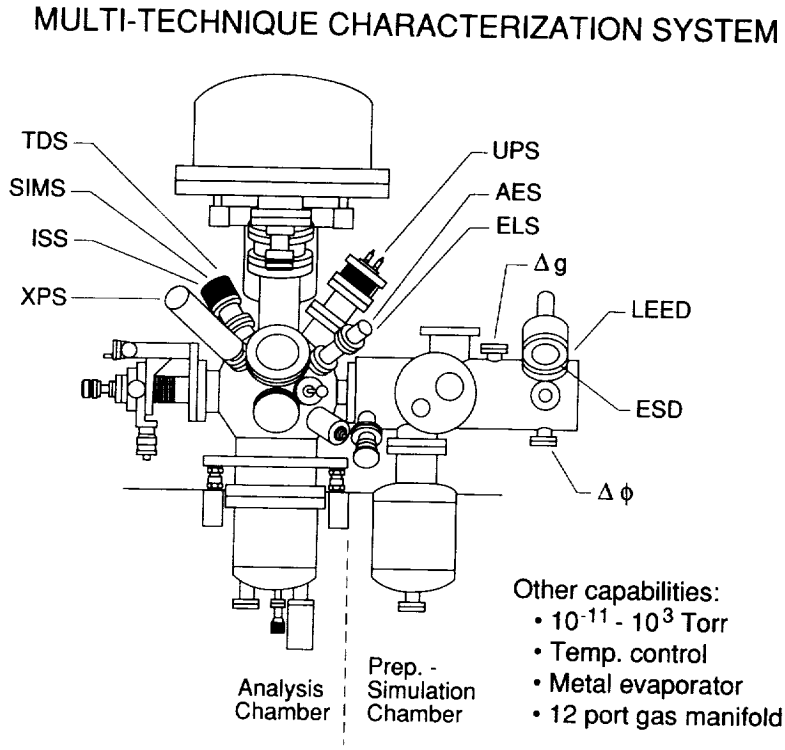

Figure 1. Schematic of the multi-technique surface analytical facility used to characterize sensor materials and processes.

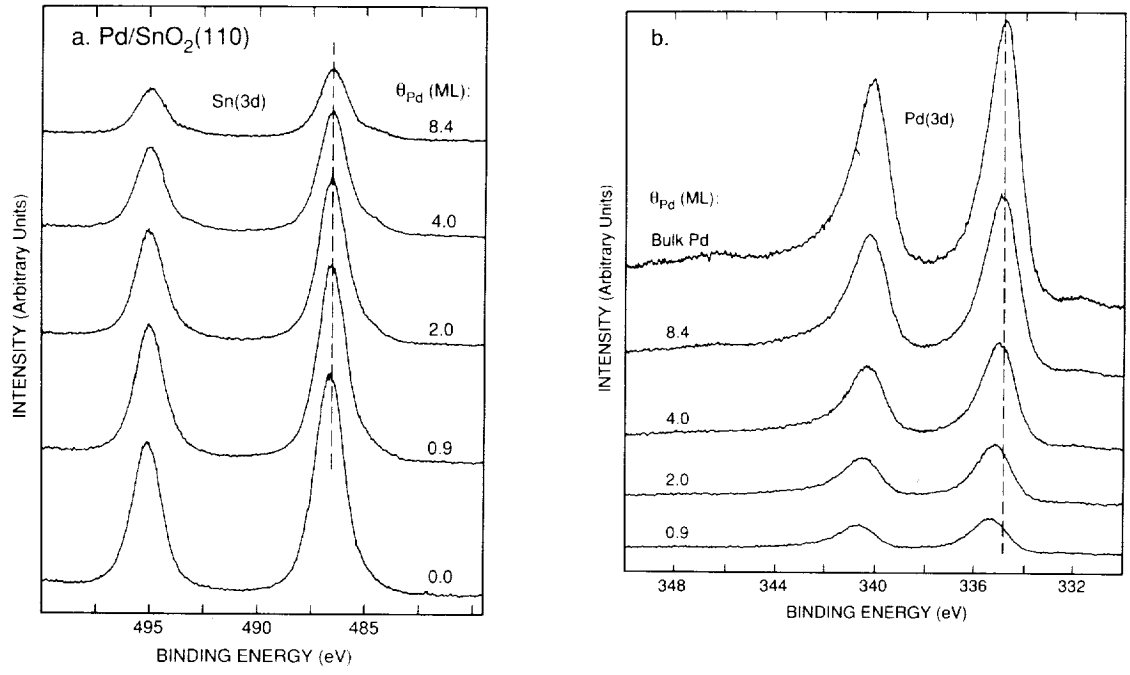

Figure 2. XPS core level (a) Sn 3d and (b) Pd 3d spectra for various Pd coverages on oxidized SnO_2(110).

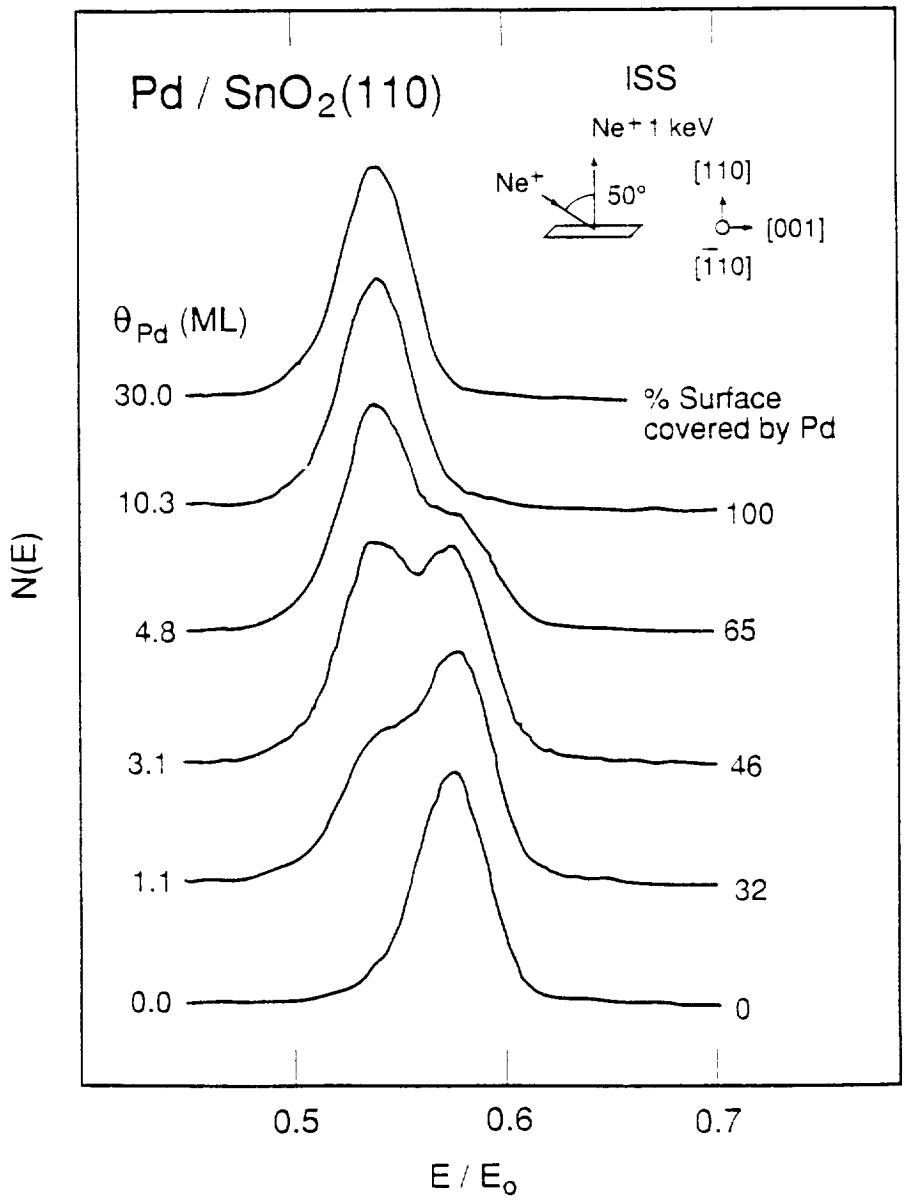

Figure 3. Ne^+ ISS spectra for various coverages of Pd on oxidized $SnO_2(110)$. E_0 = 1000 eV. Spectra are not drawn to scale.

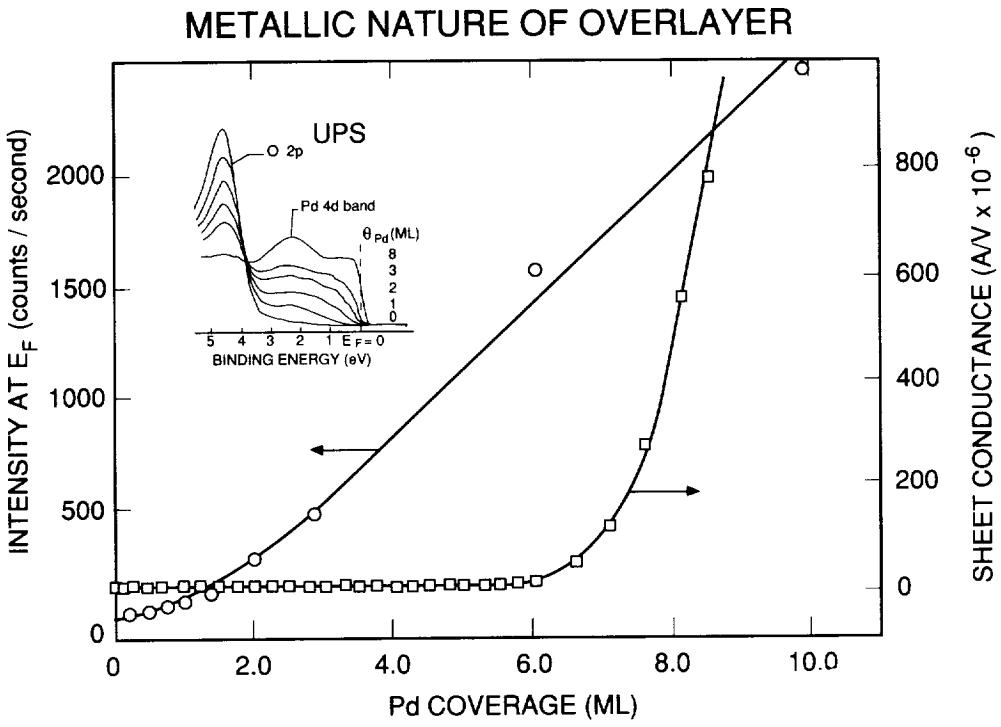

Figure 4. UPS photoelectron intensity at the Fermi level, $N(E_F)$, and 4-point conductance as a function of Pd coverage for deposition on oxidized SnO_2(110).

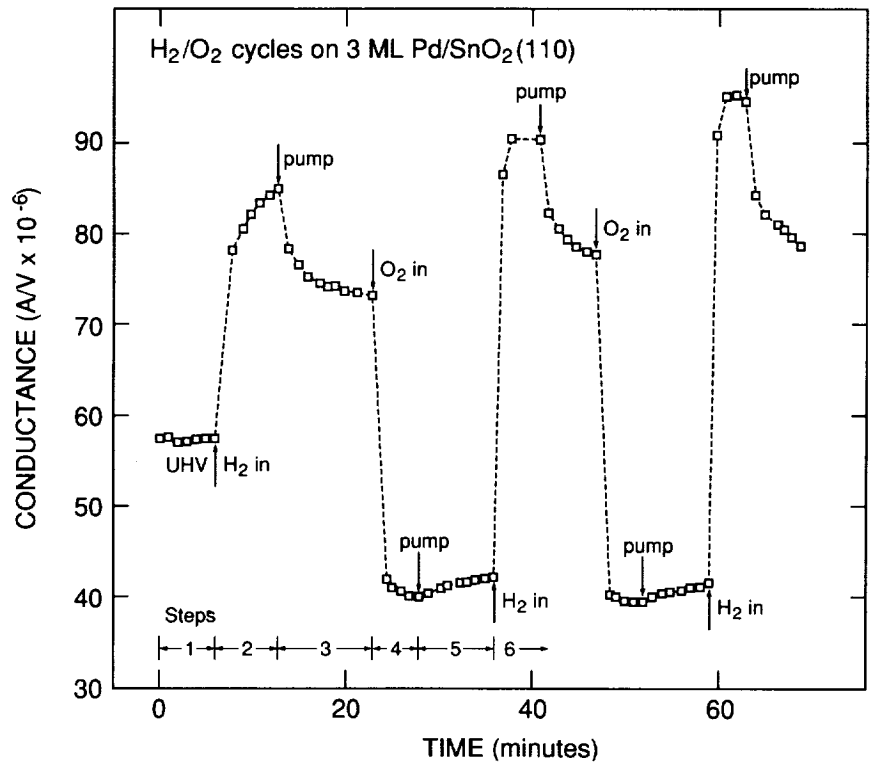

Figure 5. Conductance versus time for sequential hydrogen and oxygen exposures of the 3 ML Pd/SnO_2(110) surface at 400K. All gas exposures were performed at a constant pressure of 10^{-5} mbar. Refer to text for further details.

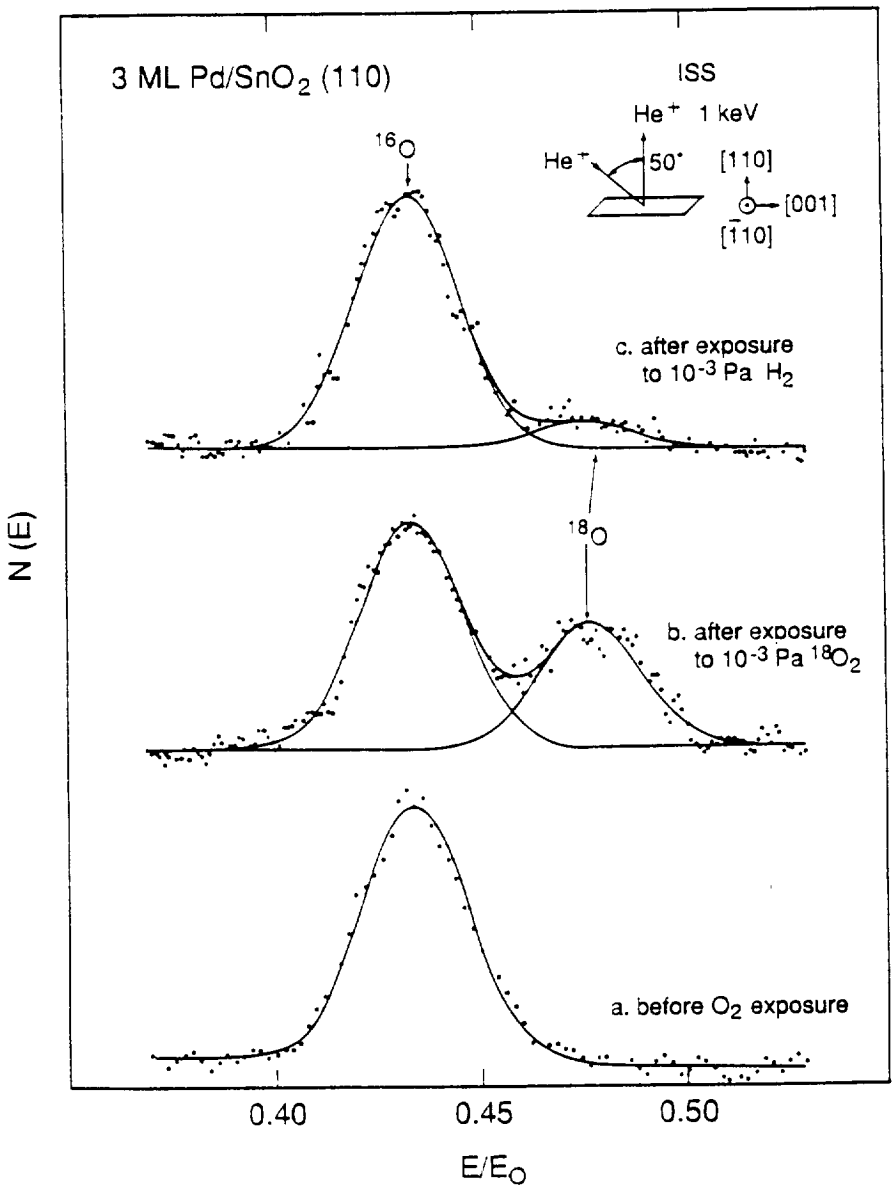

Figure 6. Ion scattering spectroscopy for 3 ML Pd/SnO_2 (110) surface after a) 500K anneal for 3 minutes in UHV; b) exposure of the surface in a) to 10^{-5} mbar $^{18}O_2$ at 400K for 5 minutes; and c) exposure of the surface in b) to 10^{-5} mbar H_2 at 400K for 5 minutes.